Ultra-Wide Bandwidth Signal Propagation for Indoor Wireless Communications

Moe Z. Win, and Robert A. Scholtz
Communication Sciences Institute, EEB 500
Department of Electrical Engineering-Systems
University of Southern California, Los Angeles, CA 90089-2565 USA

Mark A. Barnes
Time Domain Systems, Inc.
6700 Odyssey Drive, Suite 100, Huntsville, AL 35806 USA

Abstract— **An ultra-wide bandwidth (UWB) signal propagation experiment is performed in a typical modern office building in order to characterize the UWB signal propagation channel. The bandwidth of the signal used in this experiment is in excess of one GHz. Robustness of the UWB signal to fades is quantified through histogram and cumulative distribution of the received energy in various locations of the building. The results show that UWB signal does not suffer fades.**

I. Introduction

PROPAGATION environments place fundamental limitations on the performance of wireless communications systems. The existence of multiple propagation paths (multipath), with different time delays, give rise to complex, time-varying transmission channels. A line-of-site path between the transmitter and receiver seldom exists in indoor environments, because of natural or man-made blocking, and one must rely on the signal arriving via multipath.

Many propagation measurements have been made over the years on both indoor and outdoor channels with much "narrower bandwidths" [1], [2], [3], [4], [5], [6], [7], [8], [9], [10], [11], [12], [13], [14], [15], [16], [17], [18]. A comprehensive reference on the indoor propagation channels (a total of 281 references) can be found in the tutorial survey paper by Hashemi [9]. Some of the work by Rappaport [1], [2], [3], [4], [5] and others are listed here as selected references [6], [7], [8]. Although the research described in this paper does not cover outdoor propagation channels, the classic works on outdoor propagation channels by Turin [10], [11], [12], [13], by Cox [14], [15], [16], [17], and by Nielson [18] are noted here for their excellent measurement procedures and data reduction techniques. However, these measurements are inadequate for UWB transmission systems, and characterization of UWB signal propagation channel has not been available previously in the literature. Careful characterization the UWB signal propagation channel is prudent for determining optimum methods, in order to achieve the quality communication.

The research described in this paper was supported in part by the Joint Services Electronics Program under contract F49620-94-0022, and in part by the Integrated Media Systems Center, a National Science Foundation Engineering Research Center with additional support from the Annenberg Center for Communication at the University of Southern California and the California Trade and Commerce Agency.

The corresponding author can be reached by E-mail at win@milly.usc.edu

II. Experimental Design and Measurement Apparatus

A short duration pulse, with sub-nanosecond duration, is transmitted as an excitation signal of the propagation channel. The received signal represents the convolution between the excitation pulse and the impulse response of the channel. The time varying characteristic of the channel can be observed by periodic repetition of the pulse transmission. The duration of the single pulse, inversely proportional to the bandwidth of the transmission, determines the *multipath resolution*, i.e., the minimum discernible path between individual multipath components. The period of the periodic pulse signal transmission determines the maximum observable multipath delay. Hence, successive multipath components with differential delay greater than the width of the pulse and within one period of the periodic pulse transmission can be measured unambiguously.

A block diagram of the measurement apparatus is shown in figure 2. The transmitter consists of a periodic pulse generator that transmits pulses at every 500 ns using a step recovery diode-based pulser connected to a UWB antenna. The receiver consists of a receive antenna, a trigger probing antenna, a wideband low noise amplifier (LNA), and a digital sampling oscilloscope (DSO). Multipath profiles are captured by the DSO and sent over a HPIB bus to a personal computer for storage. A probe antenna, in proximity to the transmit antenna, supplies a trigger signal to the DSO by a long fixed length coaxial cable. Therefore, all recorded multipath profiles have the same absolute delay reference, and time delay measurements of the signals arriving to the received antenna via different propagation paths can be made. During each of the multipath profile measurement, both the transmitter and receiver are kept stationary. The multipath propagation channel is frozen during the measurement time by ensuring that people in the vicinity of the transmitter and receiving antenna are

0-7803-3925-8/97 $10.00 ©1997 IEEE

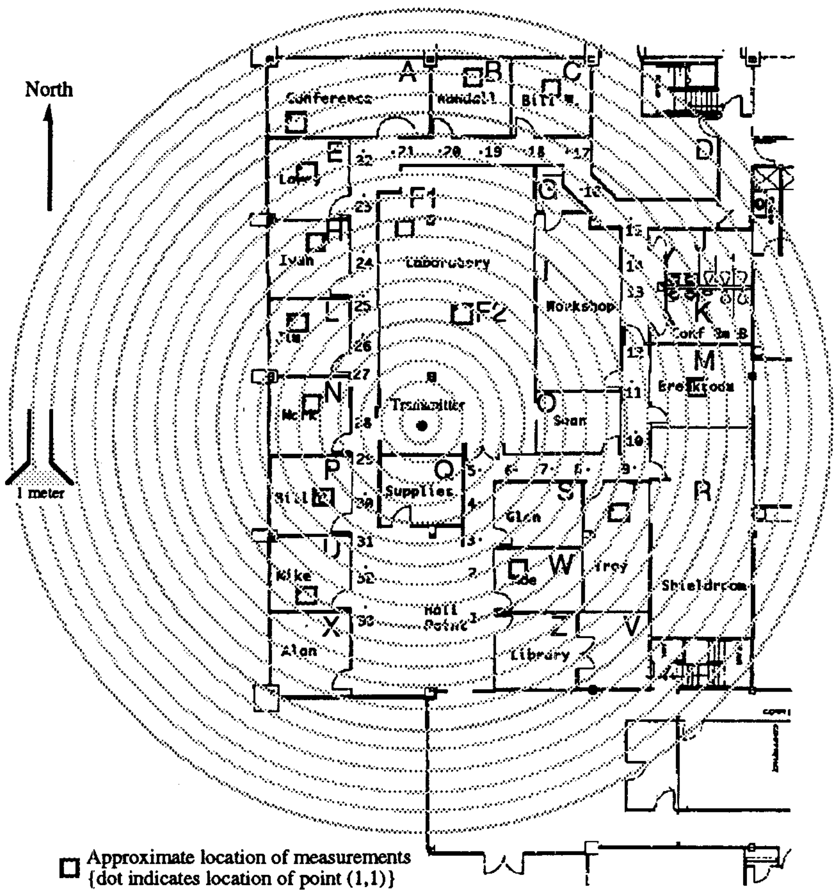

Fig. 1. The layout diagram of a typical modern office building where the propagation measurement experiment was performed. The concentric circles are centered on the transmit antenna and are a spaced at 1 meter intervals.

not moving.

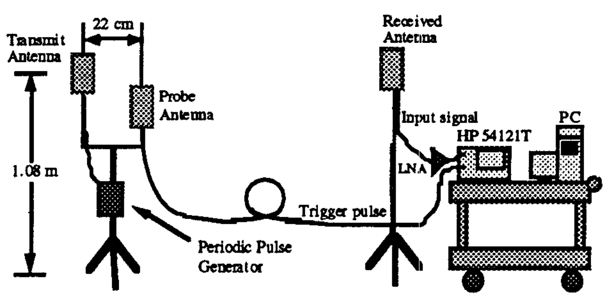

Fig. 2. A block diagram of the measurement apparatus.

III. Results

Figure 1 shows the layout of the modern office building where the propagation measurement experiment was performed. Each of the rooms is labeled alphanumerically. Walls around offices are framed with metal studs and covered with plaster board. The wall around the laboratory is made from acoustically silenced heavy cement block. There are steel core support pillars throughout the building, notably along the outside wall and two within the laboratory itself. The shield room's walls and door are metallic. The transmitter is kept stationary in the central location of the building near a computer server in a laboratory denoted by F. The transmit antenna is located 165 cm from the floor and 105 cm from the ceiling. Figure 3 shows the transmitted pulses measured by the receive antenna, located 1 m away from the transmit antenna with the same height. Measurements were made while the vertically polarized receive antenna is rotated about its axis in 45° steps. Measurements shown in figure 3 are labeled 0°, 45°, and 90°, where 0° refers to the case where the transmit and receive antennas are facing each other. Figure 3 illustrates that the radiation pattern of the antenna used in the experiment is circularly symmetric around the vertical axis. Notice from the building layout diagram given in figure 1 that the closest object to the measurement apparatus is the south wall of laboratory F, which is at least 1 meter away. The signal arriving to the receiving antenna, except the line-of-sight (LOS) signal, must travel a minimum distance of 3 meters. The initial multipaths come form floor and ceiling, 5.2 ns and 4.1 ns after the LOS signal respectively, and hence the first 10 ns of the recorded waveforms in figure 3 represent clean pulse arriving via the direct LOS path and not corrupted by multipath components.

Multipath profiles are measured at various locations in the rooms and hallways throughout the building. Specifically, data is collected at 14 different rooms and hallways. In each room, 300 ns long windows of multipath measure-

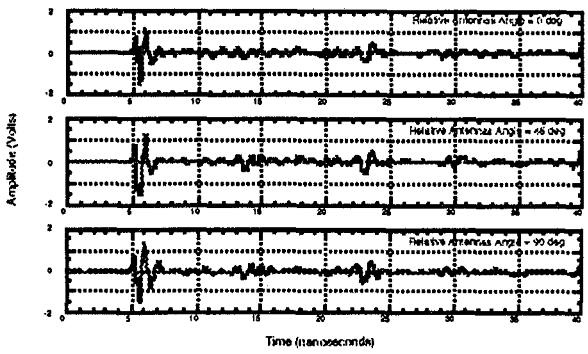

Fig. 3. Transmitted pulses measured by the receive antenna located 1 m away from the transmit antenna with the same height. Measurements were made while the vertically polarized receive antenna is rotated about its axis, where 0° refers to the case where the transmit and the received antenna are facing at each other.

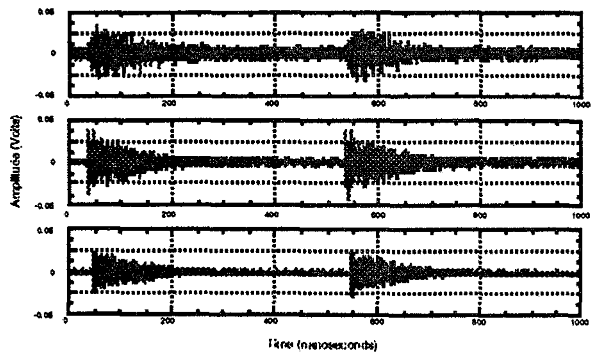

Fig. 4. Average multipath measurements of 32 sequentially measured multipath profiles where the receiver is located at the same exact locations in offices U, W and M where the measurement grids are 10, 8, and 13 meters away from the transmitter respectively.

ments are made at 49 different locations over a 3 feet by 3 feet grid. The approximate location of these measurement grids in each room are shown in figure 1. They are arranged spatially in a 7x7 square grid with 6 inch spacing. Each location on the grid is numbered as (i, j), where i represents the rows and j represents the column of the grid. As a convention, the top row is always parallel and adjacent to the north wall of the room. The received antenna is located 120 cm from the floor and 150 cm from the ceiling. This antenna height is envisioned to be typical for future indoor applications.

A single multipath profile of 1000 ns long, which captures the response of two successive probing pulses, is also made in each room. Figure 4 shows the 1000 ns long measurement, where two back to back multipath measurement cycles are captured by the receiver located in offices U, W and M respectively. The approximate distances between the transmitter and the location of these measurement grids located in offices U, W and M are 10, 8, and 13 meters respectively. Figure 4 also shows that the response of the first probing pulse has decayed (is sufficiently settled down) before the next pulse arrives at the antenna. Substantial differences in the noise floor at various locations throughout the building is observed. Specifically, the multipath profiles recorded in the offices W and M have a substantially lower noise floor compared to the profiles recorded in office U. This is explained, with the help of the building layout diagram given in figure 1, by observing: Office U is situated at the edge of the building with large glass window. Offices W and M are situated roughly in the middle of the building. Furthermore, offices W and M are adjacent to room R which is shielded from electromagnetic radiation. Interference from radio stations, television stations, cellular and paging towers, and other external electromagnetic interference (EMI) sources are attenuated by the shielded walls and multiple layers of other regular walls. The increased noise floor is generally observed for all the measurements made in offices located at edges of the building with large glass windows.

Figure 5 shows the averaged multipath profiles measured in office P at locations (4,1), (4,4) and (4,7) along the horizontal cross section of the grid with three different aligned positions of one foot apart. The approximate distance between the receiver in the office P and the transmitter is approximately 6 meters, relatively close compared to other rooms. The data that is collected in this room represents typical UWB signal transmission for the "high SNR" case. Notice that the direct path response (leading edge of the responses) suggests that the location of the receiver for the lower trace is closer to the transmitter than that of the upper trace. This fact is easily verified by building layout diagram of figure 1. Multipath delay spreads on the order of a hundred ns is observed.

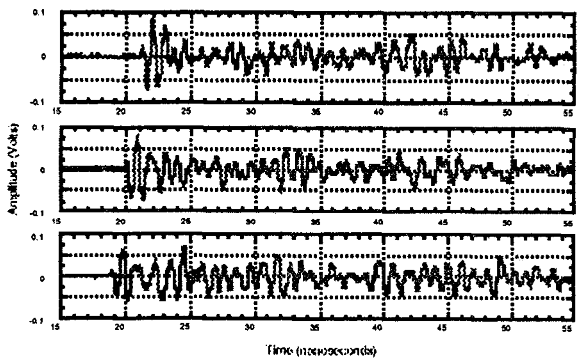

Fig. 5. Averaged multipath profiles of 50 ns window measured in office P along the horizontal cross section of the grid at three different aligned positions of one foot apart. The transmitter is approximately 6 meters from the receiver representing typical UWB signal transmission for the "high SNR" case.

To understand the effect of office doors, two multipath profiles are recorded at the same location in office B. One profile is recorded with the office door open and the other profile is recorded with the office door closed. No noticeable effect between these two measurements is observed. The effect of the large computer monitor is also considered. The receiving antenna is placed near a large computer monitor in office C and measurements are made. A slight increase in noise floor is observed when the computer monitor is on.

IV. Robustness of the UWB Signal to Fades

Robustness of the UWB signal to fades can be assessed by measuring the received energy in various locations of the building relative to the received energy at a reference point. Mathematically, the quantity *fade* at a location (i,j) can be defined as

$$F_{i,j} = 10\log_{10} E_{i,j} - 10\log_{10} E_{ref} \qquad [dB]. \qquad (1)$$

The received energy $E_{i,j}$ at a location (i,j) is given by

$$E_{i,j} = \int_0^T |r_{i,j}(t)|^2 dt, \qquad (2)$$

where $r_{i,j}(t)$ is the measured multipath at location (i,j) and T is the observation time. The reference energy E_{ref} is chosen to be the energy in the LOS path measured by the receiver located 1 meter away from the transmitter.

The quantity $F_{i,j}$ is calculated for the measurements made at 686 different locations (14 different rooms with 49 locations/room, 21 locations in the shield room, and 34 locations around the hall ways). First and second order local statistics of the total received energy are calculated. Mean and variance of the received energy collected locally over 49 spatial points (except 21 spatial points for room R, and 34 spatial points for hall ways) in each room are estimated by

$$\hat{\mu} = \frac{1}{N}\sum_{i,j} F_{i,j} \qquad (3)$$

and

$$\hat{\sigma}^2 = \frac{1}{N-1}\sum_{i,j}(F_{i,j} - \hat{\mu})^2 \qquad (4)$$

It can be shown that these estimate are a function of complete sufficient statistics if the received signal energy $E_{i,j}$ are random samples from normal families. Then by the Lehmann-Scheffé theorem [19], the estimates given by (3) and (4) are unique and gives the uniformly minimum variance unbiased estimates.

Table I shows the estimates of the mean and the variance of the received energy in each room based on 49 sample (except 21 samples for room R, and 34 samples for hall ways). The histogram and the cumulative distribution function of the received energy collected locally over 49 spatial points in each room (except 21 samples for room R, and 34 samples for hall ways) are computed and shown in figures 6 and 7 respectively. These figures along with table I indicates that the signal energy per received multipath waveform varies by at most 5 dB as received position varies over the measurement grid within the room. This clearly demonstrates the robustness of UWB signal transmission in a severe fading environments, and that UWB radio have the potential for fade-free communications even in this severe indoor multipath environment. In many situations, the transmitted power can be reduced by 10-30 dB, since only a *small fading margin* in communication link budget is required to guarantee the reliable communication of UWB radio.

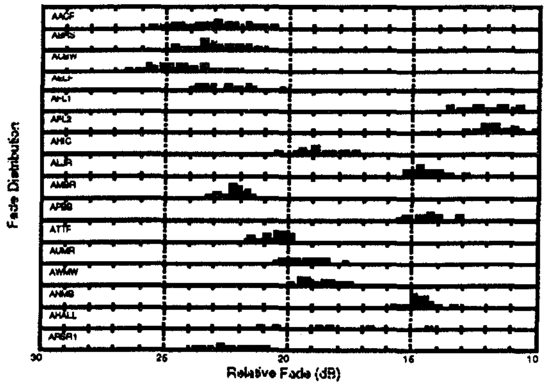

Fig. 6. The histogram received energy collected locally over 49 spatial points (except 21 spatial points for room R, and 34 spatial points for hall ways) in each room. Total of 686 energy measurements are used in this plot.

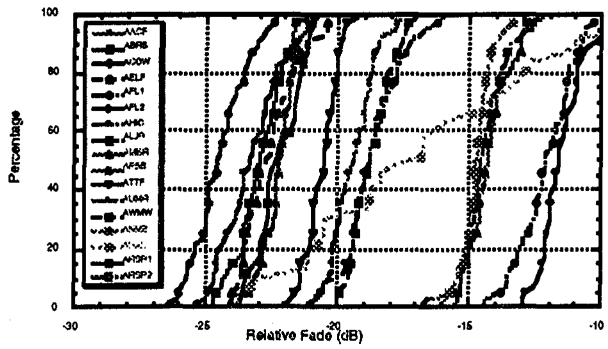

Fig. 7. The cumulative distribution function of the received energy collected locally over 49 spatial points (except 21 spatial points for room R, and 34 spatial points for hall ways) in each room. Total of 686 energy measurements are used in this plot.

V. Conclusions

Extensive UWB propagation measurements have been made in 14 different rooms and hallways of a modern office building using a periodic pulse generator that transmits UWB pulses at every 500 ns. Multipath measurements of 300 ns long window are made at 49 different locations arranged spatially in a 7x7 square grid with 6 inch spacing covering 3 feet by 3 feet. The same absolute delay reference for all recorded multipath profiles is achieved, and the time delay measurements of the signals arriving to the receive antenna via different propagation paths are made.

Increased noise floor is generally observed for all the measurements made in offices located at edges of the building with large glass windows; and is attributed to radio stations, television stations, cellular and paging towers, and other external electromagnetic interference (EMI) sources

TABLE I
FADE STATISTICS

Office	≈ distance (meters)	Minimum (dB)	Maximum (dB)	$\hat{\mu}$ (dB)	Median (dB)	$\hat{\sigma}$ (dB)	# of Samples
F2	5.5	-12.9970	-9.64586	-11.5241	-11.6813	0.8161	49
N	5.5	-16.0060	-13.2949	-14.7260	-14.7690	0.5892	49
P	6.0	-15.5253	-12.2185	-14.2373	-14.2820	0.8091	49
L	8.0	-16.6966	-12.4310	-14.4500	-14.5538	0.8342	49
W	8.5	-20.0157	-17.0351	-18.7358	-18.7425	0.7622	49
F1	9.5	-14.4064	-9.79770	-12.0986	-12.1407	1.0563	49
H	10.0	-21.0415	-16.1628	-18.7141	-18.8142	1.1240	49
U	10.0	-21.1719	-17.6232	-19.4275	-19.4092	0.8024	49
T	10.5	-21.9113	-19.2986	-20.6100	-20.5419	0.5960	49
R	10.5	-23.7221	-20.8867	-22.2675	-22.3851	0.8686	21
M	13.5	-23.8258	-20.9277	-22.2568	-22.2064	0.6439	49
E	13.5	-24.1454	-20.2000	-22.5973	-22.7824	1.0332	49
A	16.0	-25.4171	-20.7822	-23.2826	-23.3541	1.1512	49
B	17.0	-24.7191	-21.2006	-22.9837	-22.9987	0.8860	49
C	17.5	-26.4448	-22.3120	-24.4842	-24.5777	1.0028	49
Hall Ways		-23.8342	-6.72469	-16.9317	-17.3286	4.5289	34

coexisting in the same bandwidth. The effects of office doors, large computer monitors are investigated and no substantial effects are observed. Robustness of the UWB signal to fades is quantified through histogram and cumulative distribution of the received energy in various locations of the building. The results show that UWB signal does not suffer fades. Therefore, very little fading margin is required to guarantee the reliable communication.

ACKNOWLEDGMENTS

The authors wish to thank Troy Fuqua, Glenn Wolenec, Ivan Cowie, and Larry Fullerton of Time Domain Systems, and Paul Withington of Pulson Communications for several helpful discussions concerning the technology, capabilities, and signal processing of impulse signals.

REFERENCES

[1] Jorgen Bach Andersen, Theodore S. Rappaport, and Susumu Yoshida, "Propagation measurements and models for wireless communications channels," *IEEE Commun. Mag.*, vol. 33, no. 1, pp. 42–49, Jan. 1995.

[2] Theodore S. Rappaport and Clare D. McGillem, "UHF fading in factories," *IEEE J. Select. Areas Commun.*, vol. SAC-7, no. 1, pp. 40–48, Jan. 1989.

[3] Theodore S. Rappaport, "Characterization of UHF multipath radio channels in factory buildings," *IEEE Trans. Antennas Propagat.*, vol. AP-37, no. 8, pp. 1058–1069, Aug. 1989.

[4] Theodore S. Rappaport, Scott Y. Seidel, and Koichiro Takamizawa, "Statistical channel impulse response models for factory an open plan building radio communication system design," *IEEE Trans. Commun.*, vol. COM-39, no. 5, pp. 794–807, May 1991.

[5] Scott Y. Seidel and Theodore S. Rappaport, "914 MHz path loss prediction models for indoor wireless communications in multifloored buildings," *IEEE Trans. Antennas Propagat.*, vol. AP-40, no. 2, pp. 207–217, Feb. 1992.

[6] Daniel M. J. Devasirvatham, "Multipath time delay jitter measured at 850 MHz in the portable radio environment," *IEEE J. Select. Areas Commun.*, vol. SAC-5, no. 5, pp. 855–861, June 1987.

[7] Adel A.M. Saleh and Reinaldo A. Valenzuela, "A statistical model for indoor multipath propagation," *IEEE J. Select. Areas Commun.*, vol. SAC-5, no. 2, pp. 128–137, Feb. 1987.

[8] Robert J.C. Bultitude, Samy A. Mahmoud, and William A. Sullivan, "A comparison of indoor radio propagation characteristics at 910 MHz and 1.75 GHz," *IEEE J. Select. Areas Commun.*, vol. SAC-7, no. 1, pp. 20–30, Jan. 1989.

[9] Homayoun Hashemi, "The Indoor radio propagation channel," *Proc. IEEE*, vol. 81, no. 7, pp. 943–968, July 1993.

[10] G.L. Turin, Fred D. Clapp, Tom L. Johnston, Stephen B. Fine, and Dan Lavry, "A statistical model of urban multipath propagation," *IEEE Trans. on Vehicul. Technol.*, vol. VT-21, no. 1, pp. 1–9, Feb. 1972.

[11] G.L. Turin, "Introduction to spread-spectrum antimultipath techniques and their application to urban digital radio," *Proc. IEEE*, vol. 68, no. 3, pp. 328–353, Mar. 1980.

[12] Hirofumi Suzuki, "A statistical model for urban radio propagation," *IEEE Trans. Commun.*, vol. 25, no. 7, pp. 673–680, July 1977.

[13] Homayoun Hashemi, "Simulation of the urban radio propagation channel," *IEEE Trans. on Vehicul. Technol.*, vol. VT-28, no. 3, pp. 213–225, Aug. 1979.

[14] Donald C. Cox, "Delay doppler characteristics of multipath propagation at 910 MHz in a suburban mobile radio environment," *IEEE Trans. Antennas Propagat.*, vol. AP-20, no. 5, pp. 625–635, Sept. 1972.

[15] D. C. Cox, "Time- and frequency-domain characterizations of multipath propagation at 910 MHz in a suburban mobile-radio environment," *Radio Science*, , no. 12, pp. 1069–1077, Dec. 1972.

[16] Donald C. Cox, "910 MHz urban mobile radio propagation: Multipath characteristics in New York city," *IEEE Trans. Commun.*, vol. COM-21, no. 11, pp. 1188–1194, Nov. 1973.

[17] Donald C. Cox and Robert P. Leck, "Distributions of multipath delay spread and average excess delay for 910-MHz urban mobile radio paths," *IEEE Trans. Antennas Propagat.*, vol. AP-23, no. 2, pp. 206–213, Mar. 1975.

[18] Donald L. Nielson, "Microwave propagation measurements for mobile digital radio application," *IEEE Trans. on Vehicul. Technol.*, vol. VT-28, no. 3, pp. 117–132, Aug. 1978.

[19] Peter J. Bickel and Kjell Doksum, *Mathematical Statistics: Basic Ideas and Selected Topics*, Holden-Day, Inc., Oakland, California, first edition, 1995.